Accepted Manuscript

Discovery of novel Bcr-Abl^{T315I} inhibitors with flexible linker. Part 1: Confirmation optimization of phenyl-*1H*-indazol-3-amine as hinge binding moiety

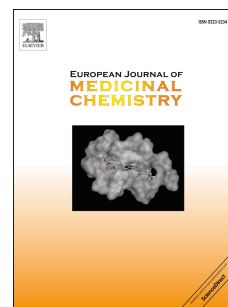Xiaoyan Pan, Liyuan Liang, Ying Sun, Ru Si, Qingqing Zhang, Jin Wang, Jia Fu, Junjie Zhang, Jie Zhang

Discovery of novel Bcr-Abl^T315I Inhibitors with flexible Linker. Part 1: Confirmation Optimization of Phenyl-*1H*-indazol-3-amine as Hinge Binding Moiety

Xiaoyan Pan[a], Liyuan Liang[a], Ying Sun[a], Ru Si[a], Qingqing Zhang[a], Jin Wang[a], Jia Fu[a], Junjie Zhang[b], Jie Zhang[a*]

[a]*School of Pharmacy, Health Science Center, Xi'an Jiaotong University, Xi'an, 710061, China*

[b]*School of Science, Xi'an Jiaotong University, Xi'an, 710049, China*

As a continuation to our previous research, a series of novel Bcr-Abl^T315I inhibitors with flexible linker were developed.

* Corresponding author. Tel/Fax: +86-29-82655451; E-mail: zhj8623@mail.xjtu.edu.cn (Jie Zhang).

Discovery of novel Bcr-Abl[T315I] Inhibitors with flexible Linker. Part 1: Confirmation Optimization of Phenyl-1*H*-indazol-3-amine as Hinge Binding Moiety

Xiaoyan Pan[a], Liyuan Liang[a], Ying Sun[a], Ru Si[a], Qingqing Zhang[a], Jin Wang[a], Jia Fu[a], Junjie Zhang[b], Jie Zhang[a,*]

[a]*School of Pharmacy, Health Science Center, Xi'an Jiaotong University, Xi'an, 710061, China*

[b]*School of Science, Xi'an Jiaotong University, Xi'an, 710049, China*

ARTICLE INFO

ABSTRACT

As a continuation to our research, a series of novel Bcr-Abl inhibitors incorporated with 6-phenyl-*1H*-indazol-3-amine as hinge binding moiety (HBM) were developed based on confirmation analysis. Biological results indicated that these compounds exhibited an enhanced inhibition against Bcr-Abl[WT] and Bcr-Abl[T315I] in kinases assays, along with improved anti-proliferative activities in K562 cell assays. In particular, compound **Y9** displayed comparable potency with that of imatinib. It potently inhibited Bcr-Abl[WT] and Bcr-Abl[T315I] kinases with IC_{50} of 0.043 μM and 0.17 μM, respectively. Furthermore, compound **Y9** inhibited the proliferation of K562 and K562R cells with IC_{50} of 1.65 μM and 5.42 μM, respectively. Therefore, 6-phenyl-*1H*-indazol-3amine as HBM, combined with flexible linker, is a successful strategy contribute to research on T315I mutant resistance, and compound **Y9** could be served as a starting point for further optimization.

* Corresponding author. Tel/Fax: +86-29-82655451; E-mail: zhj8623@mail.xjtu.edu.cn (Jie Zhang).

1. Introduction

Chronic myeloid leukemia (CML), characterized by the clonal expansion of cells carrying the Philadelphia chromosome, is a hematopoietic stem cell disease that accounts for 15-20% of all leukemia diagnosed in adults [1]. The t(9; 22) Philadelphia chromosome translation fuses the BCR gene to the c-ABL proto-oncogene resulting in a chimeric Bcr-Abl protein with constitutively activated kinase activity [2]. By recruiting the adaptor proteins such as Grb2, Bcr-Abl can activate several signaling pathways, including MAPK, PI3K-Akt, and STAT5, leading to the uncontrolled cell proliferation and CML pathogenesis [3]. Thus, Bcr-Abl represents potential therapeutic target for the development of small molecular inhibitors. The first approved Bcr-Abl inhibitor is imatinib which significantly improves clinical responses and overall survival in CML [4].

Despite the great success in clinical use of imatinib, around 15% patients can develop resistance or tolerance to this drug due to point mutations, BCR-ABL gene amplification, and overexpression of efflux transporter [5]. The second generation Bcr-Abl inhibitors, including nilotinib, dasatinib and bosutinib, were then developed (**Figure 1**) [6-8]. They could inhibit various imatinib-resistance Bcr-Abl mutants except T315I mutation which accounts for approximately 20% acquired resistance cases [9]. Pantinib, the third generation inhibitor, has recently achieved accelerated approval for the treatment of T315I resistant CML, but side effects have limited its clinical application [10, 11]. Therefore, developing novel Bcr-Abl inhibitors on the T315I mutant is one of the top priorities in CML research.
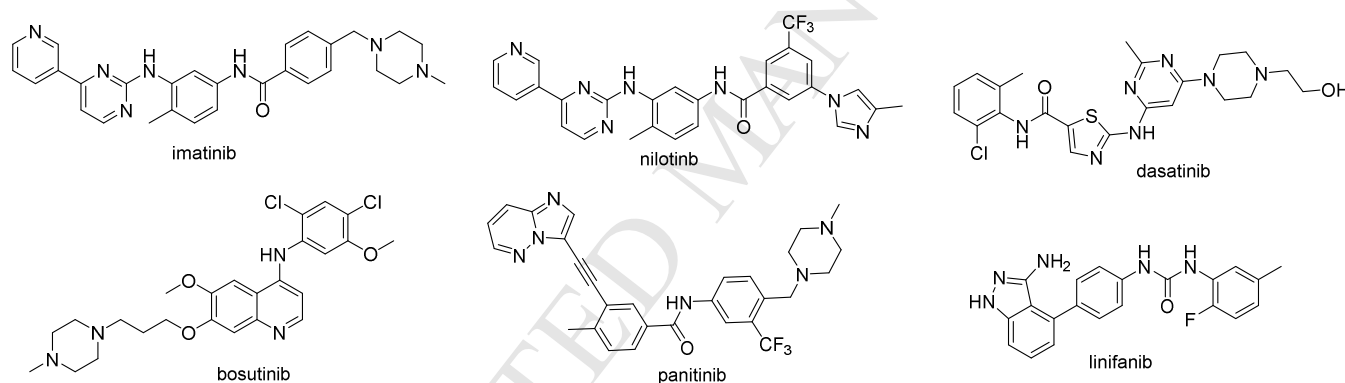

Figure 1. Development of Bcr-Abl inhibitors and multi-targeted tyrosine inhibitor linifanib.

As is known, the inhibitors reported above bind to the ATP site of Bcr-Abl to prevent substrates phosphorylated, and they belong to the type II inhibitors which target the DFG-out confirmation of tyrosine kinases [12]. According to the analysis of the interaction between those inhibitors and Bcr-Abl kinase, the pharmacophore features of type II Bcr-Abl inhibitors can be summarized as three parts, the hinge binding moiety (HBM), the linker, the selective site (DFG-out pocket) binding moiety (SBM) (**Figure 2**) [13]. Among these three pharmacophores, HBM occupies the adenine pocket and reacts with hinge region through hydrogen bonds, which is quite fatal for inhibitors' affinity. The linker, reacting with DFG motif and surrounded by

gatekeeper residue, is very important for overcoming T315I steric hindrance. Therefore, our efforts were focused on the modification of the HBM and linker to design novel Bcr-Abl^T315I inhibitors.

In our previous work, based on six-atom regulation, diacylethylenediamine and diacylpiperazine were introduced as flexible linker, affording potent Bcr-Abl inhibitors [13]. To improve the potency against Bcr-Abl^T315I, *1H*-indazol-3-amine, one fragment of Linifanib, conjugated with phenyl ring, was incorporated as new hinge binding moiety. Linfanib (**Figure 1**) is a multi-targeted ATP-competitive tyrosine kinase inhibitor, and *1H*-indazol-3-amine has received much attention as a novel

fragment to interact with the hinge region of tyrosine kinase [14]. Consequently, *1H*-indazol-3-amine conjugated with phenyl ring was validated as HBM of Bcr-Abl inhibitor (**Figure 2**), which enhanced the potency against Bcr-Abl^{T315I} for the inhibitors with diacylethylenediamine or diacylpiperazine as flexible linker [15].

As a continuation to our previous research, we investigate the effect of phenyl-*1H*-indazol-3-amine's confirmation on the affinity with Bcr-Abl. As shown in **Figure 2**, the phenyl ring is on 4-position of *1H*-indazol-3-amine, and the angle between them is almost 90 degree, making this HBM in large spatial conformation. Since the adenine pocket of Bcr-Abl prone to be a little narrow, the inhibitors, with 4-phenyl-*1H*-indazol-3-amine as HBM, may enter into the ATP pocket with high energy barrier, which may affect the activity towards Bcr-Abl. Based on

that hypothesis, the phenyl ring should be far away from indazole, making the angle smaller and more adjustable. Therefore, in order to enhance the potency, 6-phenyl-*1H*-indazol-3-amine was introduced as new HBM, adapting small spatial confirmation to enter into the ATP pocket more easily. Furthermore, we explore the effect of terminal phenyl ring with various para-substituents especially halogen substituents, as SBM, on inhibitors' activity.

In summary, Bcr-Abl^{T315I} mutation is still a major challenge for CML treatment. Herein, we described the design, synthesis and biological evaluation of a novel class of Bcr-Abl inhibitors bearing 6-phenyl-*1H*-indazol-3-amine as HBM and para-substituted phenyl ring as SBM. Moreover, *N,N'*-diacylpiperazine or *N,N'*-diacylethylene-diamine was still applied as flexible linker to reduce steric clash of Bcr-Abl^{T315I}.
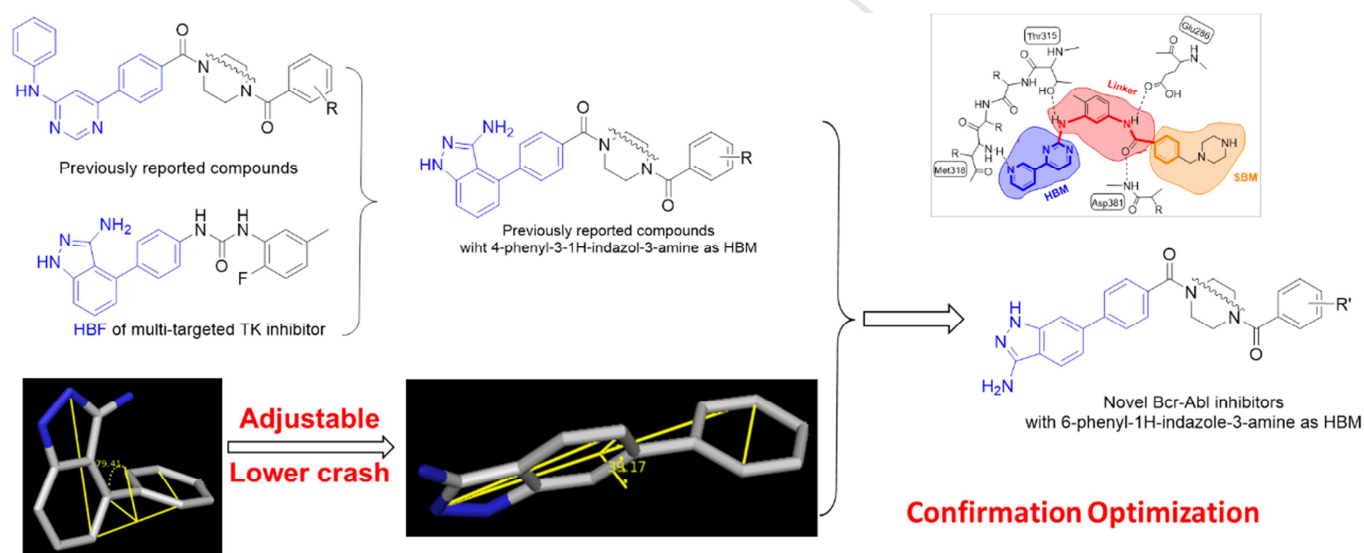

Figure 2. Design strategy and structure of novel Bcr-Abl inhibitors as anti-leukemia agents.

2. Chemistry

The general synthetic procedure for the target compounds was outlined in **Scheme 1**. There were two types of key intermediates employed to afford the title compounds. One was halogenated indazolamide (**3** and **4**). Another was diaryl ethylenediamine (**2a**-**2e**) or diaryl piperazine (**6a**-**6e**). The key intermediate **3** was prepared from commercially available 2-fluoro-6-iodobenzonitrile by using ten equiv of hydrazine monohydrate in refluxing ethanol in the presence of NaHCO$_3$ [16]. While

intermediate **4** was obtained from 4-bromo-2-fluorobenzonitrile reacting with hydrazine monohydrate in refluxing 1-butanol [17]. For the synthesis of intermediates (**2a**-**2e**) and (**6a**-**6e**), monoacylation of symmetric amines was used as the key step. In our previous work, benzoic acid was activated by CDI under solvent-free condition, followed by reaction with ethylenediamine or piperazine to generated monoacylated products [18]. This method was good for benzoic acid with low melting point. When it comes to benzoic acid with high melting point, especially

benzoic acid with substituents at *para* position, this method can't work very well or even had no product. Therefore, in order to expand the benzoic acid diversity and simplify the experiment operation when doing monoacylation of symmetric amines, new synthesis methods were developed with more stable and universal reaction condition. In terms of monoacylation of ethylenediamine, CDI was continued to be used as activating reagents, but various reaction conditions were explored with different solvents such as THF, DCM, ACN and so on. Consequently, acetonitrile was the best reaction solvents with high yield of product (**1a**-**1e**) and minimal bisadduct [19]. For piperazine monoacylation, trimethylacetyl chloride was used as activating reagent, to generate trimethylacetic arylcarboxylic anhydride from various benzoic acids in the presence of triethylamine. The anhydrides were further treated with piperazine in ethanol to provide monoacylated products (**5a**-**5e**) [20]. Next, compounds (**1a**-**1e**) or (**5a**-**5e**) reacted with 4-boronobenzoic acid, using PyBOP as condensation reagents and DMF as solvents, to get the key intermediates (**2a**-**2e**) and (**6a**-**6e**). Finally, aminoindazole **3** or **4** was coupled with diaryl ethylenediamine (**2a**-**2e**) or diaryl piperazine (**6a**-**6e**), using classical Pd-catalyzed Suzuki coupling reaction [21], to afford the title compounds **Y1**-**Y5**, **Y6**-**Y10**, **Y11**-**Y15** and **Y16**-**Y20**. All the title compounds were characterized by ^{1}H NMR, ^{13}C NMR, mass spectroscopy, melting point, MS, and HRMS data. Detailed synthetic procedures are described in the Experimental Section.
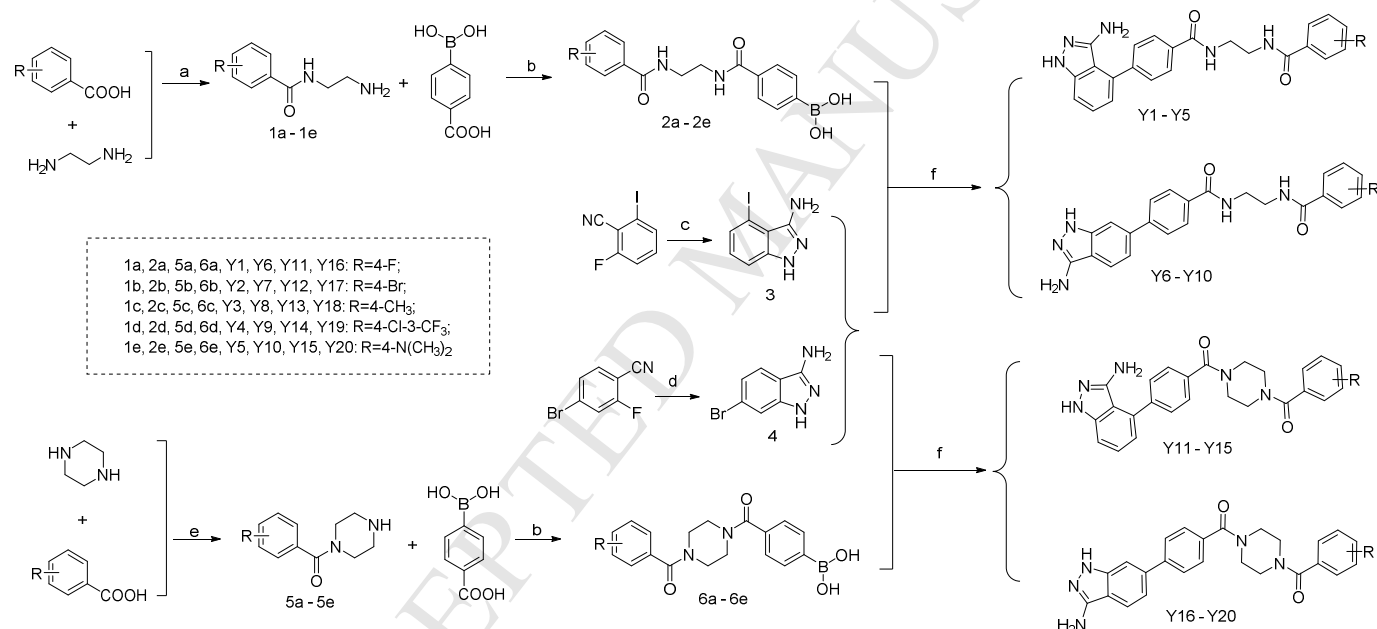
Scheme 1. Synthesis route of the title compounds (**Y1**-**Y20**). *Reagents and conditions*: a. CDI, CH_3CN, r.t.; b. PyBOP, TEA, DMF; c. $NH_2NH_2 \cdot H_2O$, $NaHCO_3$, EtOH, reflux; d. $NH_2NH_2 \cdot H_2O$, 1-butanol, reflux; e. Et_3N, CH_2Cl_2, EtOH, r.t.; f. $Pd(PPh_3)_4$, Cs_2CO_3, CH_3CN/H_2O (V:V= 3:2), 90ºC.

3. Results and discussion

All the title compounds were evaluated for their enzymatic inhibition against both Bcr-Abl[WT] and Bcr-Abl[T315I] as well as K562 cellular activities. The tyrosine kinase inhibitory potency was assayed by using the well-established ADP-Glo assays [22]. The antiproliferative potency was identified *in vitro* against Bcr-Abl positive K562 cells by using MTT method with imatinib as positive control [23].
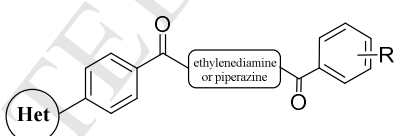
In vitro kinase inhibition and antiproliferative potency of all the title compounds were depicted in **Table 1**.

According to our previous research, with 4-phenyl-*1H*-indazol-3-amine as HBM, the *o*- or *p*- substituents on the terminal phenyl ring was favorable for compounds' activity. Taken steric hindrance into consideration, *p*-substituents were further diversified and investigated (**Y1**-**Y5** and **Y11**-**Y15**). As shown in **Table 1**, most of the title

compounds with 4-phenyl-*1H*-indazol-3-amine as HBM values confirmed an improved potency of most compounds could retain comparable potency against Bcr-Abl^{WT} and Bcr-Abl^{T315I} when alkyl and halogen substituents were introduced to *p-* position on terminal phenyl ring. Specially, compounds **Y3** and **Y12** displayed good potency against both WT and T315I Bcr-Abl kinases. For Bcr-Abl^{WT} inhibitory assays, compounds **Y4** and **Y15** were the most potent in each series with IC$_{50}$ values of 0.11 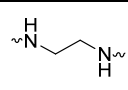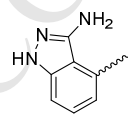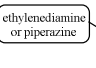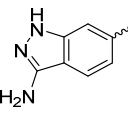and 4.28 μM, respectively. When it comes to Bcr-Abl^{T315I} assays, most compounds exhibited moderate to good activity. In particular, compounds **Y3**, **Y12** and **Y14** had good inhibition potency with IC$_{50}$ values under micromolar level. Overall, biological evaluation indicated that, with *1H*-indazol-3-amine as hinge binding fragment, the activities of this chemotypes was durable to the diversification of *p*-substituents on terminal phenyl ring. Importantly, the further modification was focus on the confirmation of phenyl-*1H*-indazol-3-amine as HBM, and the phenyl ring was changed from 4-position to 6-position in indazole, with *p*-substituents invariant (**Y6**-**Y10** and **Y16**-**Y20**). As depicted in **Table 1**, the observed IC$_{50}$

with respect to both Bcr-Abl^{WT} and Bcr-Abl^{T315I}. In particular, compound **Y9** displayed comparable potency with that of imatinib. With ethylenediamine as linker, compounds **Y6**-**Y10** had better inhibition potency than other three series against Bcr-Abl^{WT}, with IC$_{50}$ value from 0.043 to 3.45 μM. Besides, compound **Y9** and **Y10** displayed excellent activity against Bcr-Abl^{T315I}, comparable to that of imatinib. For compounds **Y16**-**Y20**, with piperazine as linker, all compounds had IC$_{50}$ values under micromolar level in kinase inhibitory assays, except for compound **Y18** toward Bcr-Abl and compound **Y17** against T315I mutant. Consequently, in comparison to **Y1**-**Y5** and **Y11**-**Y15**, these title compounds with 6-phenyl-*1H*-indazol-3-amine as HBM exhibited 10- to 100- fold increase in potency against Bcr-Abl^{WT} and Bcr-Abl^{T315I} kinases. In addition, halogen substituent 4-Cl-3-CF$_3$ was the most beneficial group for enzymatic inhibition against WT and T315I Bcr-Abl kinases.

Table 1 Structures and biological activities of title compounds (IC$_{50}$, μM).

Compd	Linker	Het	R	Abl^{WT} IC$_{50}$(μM)	Abl^{T315I} IC$_{50}$(μM)	K562 IC$_{50}$(μM)
Y1			4-F	1.35	38.53	9.49
Y2			4-Br	31.61	94.84	>150
Y3			4-CH$_3$	0.52	5.17	5.93
Y4			4-Cl-3-CF$_3$	0.11	20.00	17.08
Y5			4-N(CH$_3$)$_2$	5.75	76.76	>150
Y6			4-F	2.45	61.20	13.42
Y7			4-Br	2.16	2.68	14.04
Y8			4-CH$_3$	0.38	4.30	1.45
Y9			4-Cl-3-CF$_3$	0.043	0.17	1.65
Y10			4-N(CH$_3$)$_2$	3.45	0.29	7.52

5

Compound	Substituent			
Y11	4-F	17.56	20.86	101.83
Y12	4-Br	7.12	1.50	9.25
Y13	4-CH$_3$	5.85	178.66	>150
Y14	4-Cl-3-CF$_3$	10.66	2.08	4.90
Y15	4-N(CH$_3$)$_2$	4.28	86.06	>150
Y16	4-F	2.34	8.60	39.11
Y17	4-Br	6.28	31.90	11.30
Y18	4-CH$_3$	32.25	3.72	59.3
Y19	4-Cl-3-CF$_3$	1.99	5.33	4.84
Y20	4-N(CH$_3$)$_2$	2.54	6.23	61.16
imatinib		0.054	0.28	4.26

Furthermore, we investigated the kinase selectivity of the most potent compound (**Y9**) against other three kinases including Src, Hck and p38α for its selective profile. The results were summarized in **Figure 3**. The results revealed that compound **Y9** showed less potency against Hck, while it exhibited some inhibitory activity against p38α and Src kinases with IC$_{50}$ value of 34.5 μM and 15.1 μM, respectively. It was demonstrated that this inhibitor exhibited a good selectivity for Bcr-Abl relative to other three kinases. In addition, because of the inhibiton potency of compound **Y9** against p38α, especially Src kinases, we speculated that it may cause some inconsistency of Bcr-Abl inhibition and CML cells growth inhibition in the following anti-proliferation assays.
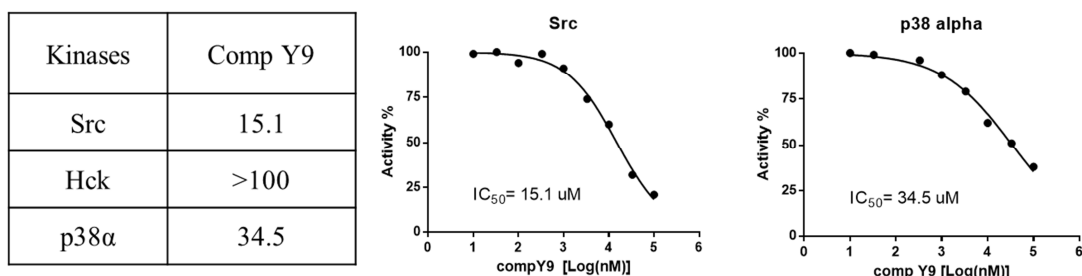
Figure 3. Kinases selectivity profile of compound **Y9** (IC$_{50}$, μM).

Next, we investigated the growth inhibition of these title compounds against Bcr-Abl positive K562 cells, and the results were also presented in **Table 1**. The majority of them displayed moderate to high antiproliferative activities. Specially, compounds **Y8** and **Y9** were more potent than imatinib with IC$_{50}$ values of 1.45 and 1.65 μM, respectively. Meanwhile, the activities of compounds **Y14** and **Y19** were comparable to that of imatinib, with IC$_{50}$ values of 4.90 μM and 4.84 μM. In accordance with the kinase inhibitory results against Bcr-Abl, compounds with phenyl ring on 6-position of indazole exhibited better antiproliferative activities than that of those corresponding compounds with phenyl ring on 4-position. Interestingly, it was found that compounds bearing N(CH$_3$)$_2$ substituent (**Y5**, **Y15** and **Y20**) displayed little inhibitory activities toward K562 cells, although they had good potency against Bcr-Abl kinases. We presumed that the N(CH$_3$)$_2$ group had been protonated in buffer, resulting in poor membrane permeability for these compounds in cell assays. Consequently, their poor permeability lead to little effect

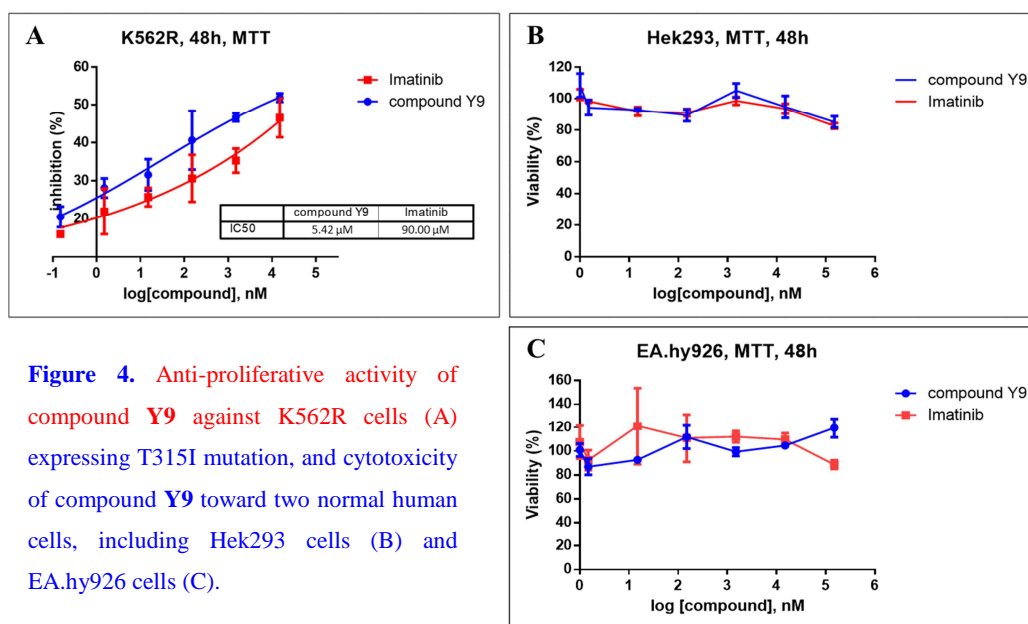on K562 cells proliferation. Above all, phenyl ring on 6-position of indazole was more favorable for antiproliferative activities than 4-position.

Figure 4. Anti-proliferative activity of compound **Y9** against K562R cells (A) expressing T315I mutation, and cytotoxicity of compound **Y9** toward two normal human cells, including Hek293 cells (B) and EA.hy926 cells (C).

Having demonstrated the potent inhibition of Abl kinases and anti-proliferative activity, compound **Y9** was further evaluated for its activity toward K562R cells expressing T315I mutation [24], with Imatinib as positive control. The results was displayed in **Figure 4A**, and compound **Y9** was found to potently inhibit the growth of K562R cells with IC_{50} value of 5.42 μM, while Imatinib has an IC_{50} value of 90.00 μM toward K562R cells. In addition, we identified the cytotoxicity of compound **Y9** on two normal cells, including Hek293 (human embryonic kidney 293 cells) and EA.hy 926 (human vascular endothelial cells), with Imatinib as control. As shown in **Figure 4B** and **4C**, compound **Y9** exhibited less toxicity toward these two cell lines when its concentration increased up to 150 μM. In summary, compound **Y9** displayed selectivity growth inhibitory activity against Bcr-Abl positive K562 and K562R cells compared to normal human cell lines.

We further evaluated the effect of compound **Y9** on the expression level and phosphorylation of Bcr-Abl in K562 cells using western blot assay. The results was shown in **Figure 5**. It was found that compound **Y9** does-dependently decreased the phosphorylation of Bcr-Abl in K562 cells compared with the negative control group, while the expression level of Bcr-Abl was unchanged. Our

findings suggested that the influence of compound **Y9** on cell viability of K562 might be attributed to the down regulation of Bcr-Abl phosphorylation. In addition, although compound **Y9** exhibit potent inhibitory activity against K562 cells compared with imatinib, it just lead a modest decrement of Bcr-Abl phosphorylated level in this assay. This finding suggested that compound Y9 might take effect through other signal pathway besides targeting Bcr-Abl, which need to be further explored in our undergoing work.
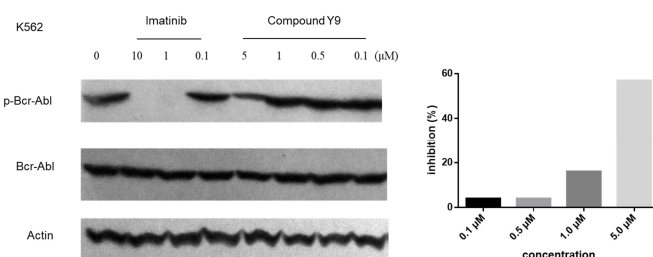

Figure 5. The effect of compound **Y9** on the phosphorylated level of Bcr-Abl in K562 cells.

To gain a better understanding of the interaction between compound **Y9** and kinases protein, molecular docking studies was conducted using Sybyl-X (Version 2.0, Tripos Inc. St. Louis, MO) [25]. Crystal structures of Bcr-Abl[WT] (PDB IP: 1IEP) and Bcr-Abl[T315I] (PDB IP: 3QRJ) [26, 27],
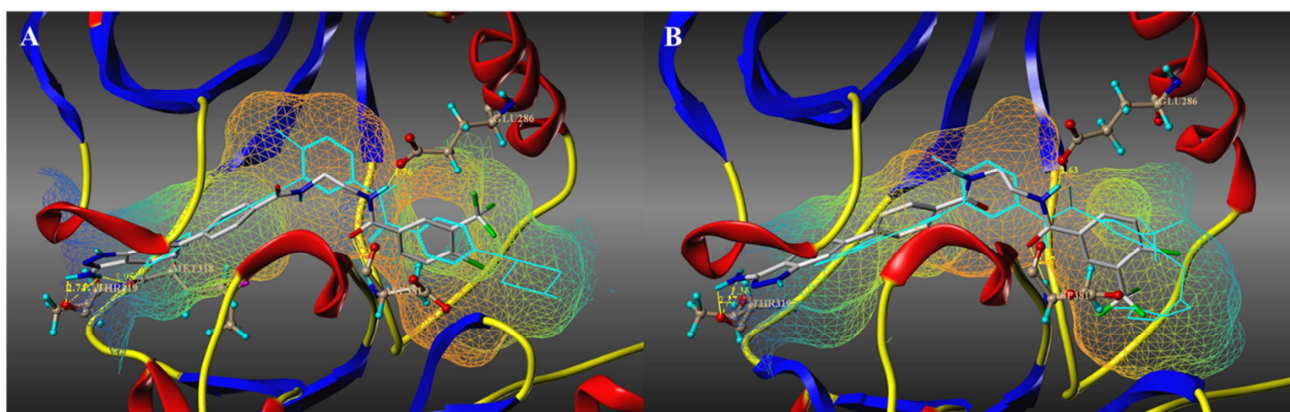
Figure 6. The binding mode of compound **Y9** with Bcr-Abl^{WT} (A) and Bcr-Abl^{T315I} (B), imatinib (A, cyan) and panitinib (B, cyan) were used as control molecule for Bcr-Abl^{WT} and Bcr-Abl^{T315I} docking, respectively.

As shown in **Figure 6A**, compound **Y9** bound across the ATP-binding site of Bcr-Abl^{WT} through five hydrogen bonds. The N-H$_2$ of *1H*-indazol-3-amine, as hydrogen bond donor, formed three hydrogen bonds with hinge region residues. One N-H formed two hydrogen bonds with Thr319 and Met318 with length of 2.70Å and 1.95Å, respectively. The other N-H formed one hydrogen bond with Thr319 with distance of 2.74Å. The conversed Asp381 of DGF motif generated one hydrogen bond with the terminal carbonyl oxygen in linker part with the length of 2.09Å. Furthermore, Glu286 of α-helix, as receptor, formed one hydrogen bond with the N-H of terminal amide group, and the distance was 1.76Å. As for Bcr-Abl^{T315I} binding, the results was displayed in **Figure 6B**. The two hydrogen atom of amine in indazole interacted with Thr319 to generate two hydrogen bonds, and the bond length was 2.27Å and 2.36Å, respectively. Other two hydrogen bonds were same as that of its binding to wild type. One hydrogen bond was generated between the carbonyl group of Glu286 and the N-H of terminal amide in linker part, and its distance was 1.63Å. The other hydrogen bond was formed between the N-H in backbone of Asp381 and the carbonyl of terminal amide group with bond length of 2.07Å. Based on above docking analysis, it was found that the binding mode of compound **Y9** with Abl kinases were similar as imatinib binding to Bcr-Abl^{WT}

and panitinib to Bcr-Abl^{T315I}, respectively. The terminal amide group could generated hydrogen bonds with conserved Glu286 and Asp381. Moreover, the indazole formed hydrogen bond network with hinge region residues. That may explain the potent activities of compound **Y9** toward Abl kinases.

For compounds with piperazine as linker, we also did *in silico* docking to rationalize its lower potency against Abl kinases compared with those compounds with ethylene-diamine as linker. The most potent compound **Y19** was used to do this study. For Bcr-Abl^{WT} docking, the results was depicted in **Figure 7A**, and there were two hydrogen bonds between them. The hydrogen atom of amine in indazole ring formed one hydrogen bond with Thr319, and the other one with Met318, for the bond length of 2.72Å and 1.92Å, respectively. For Bcr-Abl^{T315I}, the binding interactions of compound **Y19** was shown in **Figure 7B**, with two hydrogen bonds as follows: 1) the first forming between N atom of indazole ring and NH$_2$ group of Met318, the distance was 1.78Å, 2) the second forming between N-H inside indazole ring and carbonyl group in backbone of Glu316 with length of 2.18Å. Overall, the binding mode of compound **Y19** were similar as imatinib with Bcr-Abl^{WT} and panitinb with Bcr-Abl^{T315I}, respectively. However, compared with **Y9** docking results, there was no hydrogen bonds between terminal amide of

compound **Y19** and DFG motif or conserved Glu286, as linker had lower kinase activities.

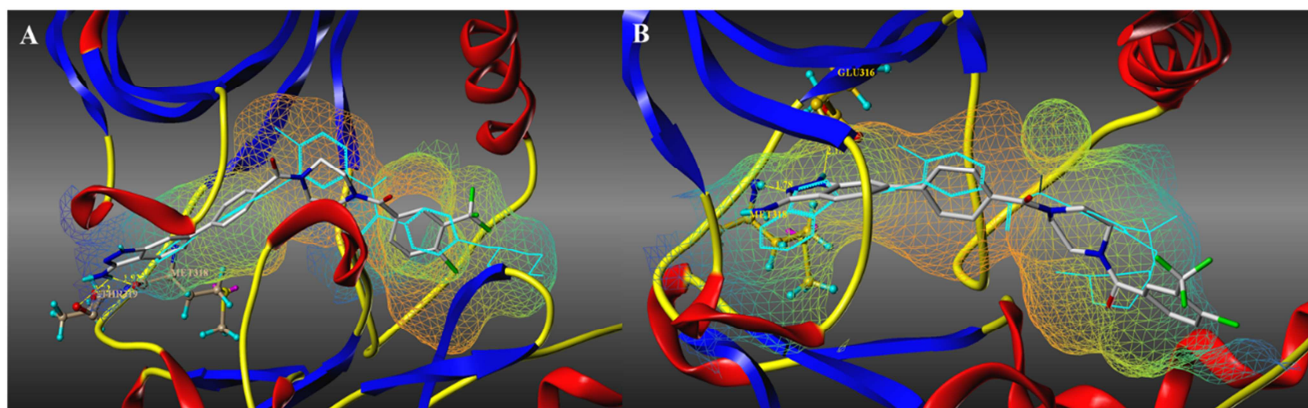which may explain why these compounds with piperazine

Figure 7. The binding mode of compound **Y19** with Bcr-Abl[WT] (A) and Bcr-Abl[T315I] (B), imatinib (A, cyan) and panitinib (B, cyan) were used as control molecule for Bcr-Abl[WT] and Bcr-Abl[T315I] docking, respectively.

Furthermore, in order to investigate the effect of phenyl position on the binding of *1H*-indazol-3-amine with hinge region, compounds **Y4** and **Y9** were performed docking using Surflex-dock module of Sybyl-X 2.0, with Bcr-Abl[WT] as target protein. As shown in **Figure 8A**, both compounds applied similar mode to bind with Bcr-Abl kinase, and *1H*-indazol-3-amine in both core structures generated hydrogen bonds with hinge region residues. However, the pyrazoles' direction differed between compounds **Y4** and **Y9** under the effect of phenyl ring position. We speculated that this may lead to different binding situations from perspective of energy crash. To visualize the energy situation between molecules and

kinase protein, Glide docking module of Schrödinger was applied to do the analysis [28]. As depicted in **Figure 8B**, 4-phenyl-*1H*-indazol-3-amine in compound **Y4** had a certain degree of steric crashes with surrounding residues including Leu248, Tyr253 and Met318. As for compound **Y9**, from **Figure 8C**, 6-phenyl-*1H*-indazol-3-amine have little crash with Leu248, even no crash with Tyr253 especially Met318 in hinge region. Through the comparison between two energy situations of compounds **Y4** and **Y9** in the hinge region, 6-phenyl-*1H*-indazol-3-amine was more favorable structure as HBM for these chemotype inhibitors with flexible linker.
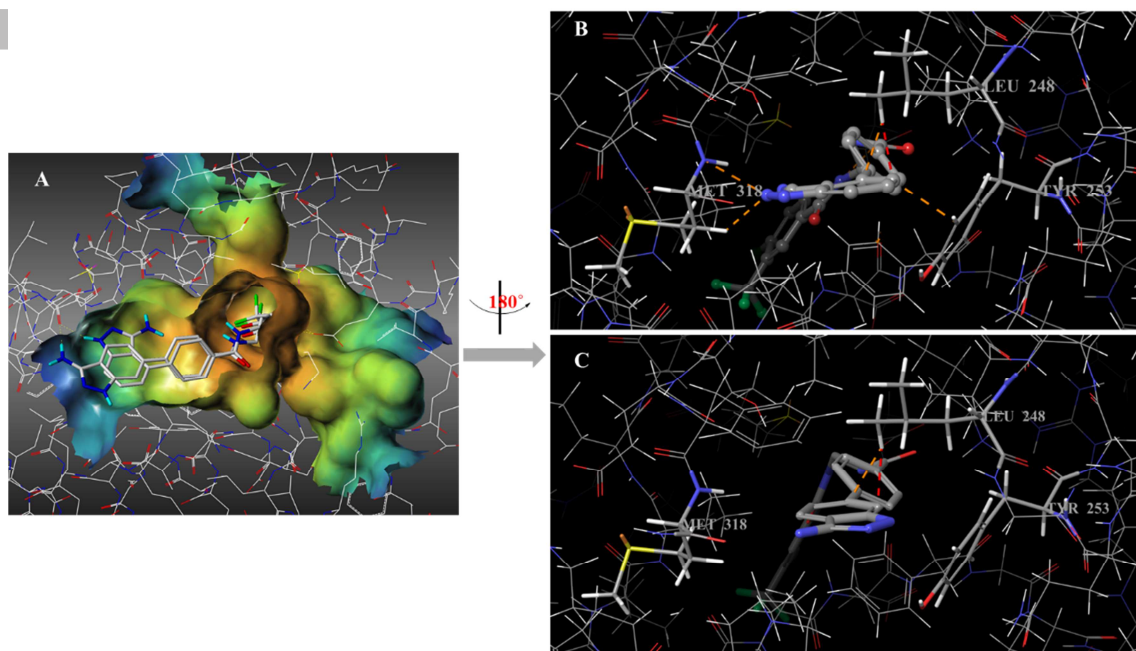
Figure 8. The docking results of compound **Y4** and **Y9** with Bcr-Abl (A), and the visualized energy situation of compounds **Y4** (B) and **Y9** (C) with surrounding residues. The orange dash bonds represent bad crash, and the red dash bonds correspond to ugly crash.

4. Conclusion

Herein, we described the continuous optimization of previously disclosed Bcr-Abl inhibitors bearing 4-phenyl-*1H*-indazol-3-amine as HBM. The effort was focus on confirmation optimization of phenyl-*1H*-indazol-3-amine interacting with the hinge region. The strategy was to transfer phenyl ring from 4-position to 6-position of indazole, far away from pyrazole, resulting in the structure more adjustable to generate favorable binding mode with lower energy barrier. Finally, a series of compounds with 6-phenyl-*1H*-indazol-3-amine as HBM, and corresponding compounds with previous reported indazol-3-amine structure used as comparison, were synthesized and evaluated. The biological results indicated that most designed compounds had an enhanced effect in kinase and cell assays, especially that compound **Y9** displayed potent inhibition against both Bcr-Abl^{WT} and Bcr-Abl^{T315I}, comparable to that of imatinib. Meanwhile, it exhibited the excellent antiproliferative activity toward Bcr-Abl positive K562 and K562R cells, better than imatinib. Moreover, using molecular modeling, it was rationalized that modification of phenyl-*1H*-indazol-3-amine confirmation could improve the affinity of Bcr-Abl inhibitors with hinge region. In particular, compound **Y9** fit well to ATP pocket

of Bcr-Abl^{WT} and Bcr-Abl^{T315I} with five or four hydrogen bonds, respectively. Furthermore, visualized energy situations analysis between phenyl-*1H*-indazol-3-amines and hinge region residues indicated that phenyl ring at 6-position led to lower crash with surroundings, more favorable for binding in ATP pocket. Besides, as described previously, diacylpiperazine especially diacylenediamine reduce the steric clash with gatekeeper residues of Bcr-Abl^{T315I}. Therefore, 6-phenyl-*1H*-indazol-3-amine as HBM, combined with flexible linker, is a successful strategy contribute to the research on T315I mutant resistance. Finally, compound **Y9**, displaying promising enzymatic inhibition as well as antiproliferative potency, could be considered as valuable starting point for further effort.

5. Experimental section

5.1. Chemistry: General procedure

Reagents and solvents were purified according to the standard procedure. The reactions except those in aqueous were performed by standard techniques for the exclusion of moisture. Reactions were monitored by thin layer chromatography (TLC) on 0.25-mm silica gel plates (GF$_{254}$) and visualized with UV light. Melting points were determined on electrothermal melting point apparatus and

were uncorrected. ^{1}H NMR spectra was measured at 400 MHz on a Bruker Advance AC 400 instrument with TMS as an internal standard. Mass spectra was measured using gas or liquid chromatography mass spectrometry (GC/LC-MS) with electrospray ionization (ESI). HRMS was measured using AXIMA-CFR^{TM} MALDI-TOF-MS or micrOTOF-Q □. All compounds were purified by flash chromatography with silica gel.

5.1.1. 4-iodo-1H-indazol-3-amine (1)

2-fluoro-6-iodobenzonitrile (5.0 g, 10.1 mmol), NaHCO$_3$ (2.6 g, 31 mmol) and hydrazine monohydrate (5.0 g, 99.9 mmol) were dissolved in ethanol 60 mL. The resulting mixture was heated to reflux for 8 h. After cooling to room temperature, 50 mL water was added and the reaction mixture was allowed to stir for another 2 h at room temperature. The product was collected by filtration and dried under vacuum to give (1) as slight yellow solid (4.8 g, 92%).

5.1.2. N-(2-aminoethyl)-4-fluorobenzamide (2a)

4-fluorobenzoic acid (15 mmol), carbonyldiimidazole (2.92 g, 18 mmol) were dissolved in 60 mL anhydrous ACN, and was stirred for 1 h at room temperature. In a separate dry 50 mL round bottom flask, fitted with an addition funnel, was placed 10 mL (150 mmol) of ethylenediamine. The activated 4-fluorobenzoic acid was transferred to the addition funnel and added dropwise to the ethylenediamine. The reaction was stirred at room temperature for 3h. Then CH$_3$CN was evaporated, and 40 mL HCl solution (6 mol/L) was added to the residue. The mixture was extracted with CH$_2$Cl$_2$ (10 mL) to remove diacylated product. The aqueous layer was adjust to PH 8~9 with 10 g NaOH, and extracted with CH$_2$Cl$_2$ (30 mL×3). Then the organic solution was combined, dried over Na$_2$SO$_4$ overnight, concentrated by rotary evaporation to afford the crude product which can be directly used in the next step. EI-MS (m/z) 183[M+H]$^+$.

The intermediates **2b**-**2e** were prepared by ethylenediamine and commercially benzoic acids with different substituents using the same procedure as described above.

5.1.3. (4-((2-(4-fluorobenzamido)ethyl)carbamoyl)phenyl) boronic acid (3a)

4-carboxyphenylboronic acid (0.996 g, 6 mmol), PyBOP (3.43 g, 6.6 mmol) were dissolved in 10 mL anhydrous DMF, and anhydrous triethylamine (1.8 mL, 12 mmol) was added dropwise to the solution. After stirring at room temperature for 20 min, *N*-(2-aminoethyl)-4-fluorobenz-amide (**2a**) was added and the reaction mixture was stirred overnight at room temperature. The mixture was dissolved in 100 mL H$_2$O and then extracted with EtOAc (50 mL×3). The combined organic layer was washed with water (20 mL×3) and brine (30 mL), dried over Na$_2$SO$_4$ for overnight, filtered, and concentrated *in vacuo*. The crude product was purified by flash chromatography with PE/EtOAc (v/v = 1:5) as eluent to afford (**3a**) as white solid (1.1 g, 55%). Mp 326 □327ºC, EI -MS (m/z): 329.00 [M-H]$^-$.

The intermediate compounds **3b**-**3e** were prepared using the same procedure as described above.

5.1.4. (4-((2-(4-bromobenzamido)ethyl)carbamoyl)phenyl) boronic acid (3b)

N-(2-aminoethyl)-4-bromobenzamide (**2b**) was used as starting material to obtain **3b** (2.0 g, 86%). Mp 318□320ºC, EI-MS (m/z): 389.05 [M-H]$^-$.

5.1.5. (4-((2-(4-methylbenzamido)ethyl)carbamoyl)phenyl) boronic acid (3c)

N-(2-aminoethyl)-4-methylbenzamide (**2c**) was used as starting material to obtain **3c** (1.69 g, 87%). Mp 330□331ºC, EI-MS (m/z): 325.05 [M-H]$^-$.

5.1.6. (4-((2-(4-chloro-3-(trifluoromethyl)benzamido)ethyl) carbamoyl)phenyl)boronic acid (3d)

N-(2-aminoethyl)-4-chloro-3-(trifluoromethyl)benzamide (**2d**) was used as starting material to obtain **3d** (2.18 g, 88%). Mp 125□127ºC, EI-MS (m/z): 415.05 [M+H]$^+$.

5.1.7. (4-((2-(4-(dimethylamino)benzamido)ethyl)carbamoyl) phenyl)boronic acid (3e)

N-(2-aminoethyl)-4-(dimethylamino)benzamide (**2e**) was used as starting material to obtain **3e** (1.48 g, 69%). Mp 180□182ºC, EI-MS (m/z): 356.05 [M+H]$^+$, 354.10 [M-H]$^-$.

5.1.8. 4-(3-amino-1H-indazol-4-yl)-N-(2-(4-fluorobenz-amido) ethyl)benzamide (Y1)

In a 100 mL round bottom flask with an a condenser tube, 4-iodo-*1H*-indazol-3-amine (**1**) (0.39 g, 1.5 mmol), (4-((2-(4-fluorobenzamido)ethyl)carbamoyl)phenyl)boronic acid (**3a**) (1.8 mmol), Cs₂CO₃ (1.46 g, 4.5 mmol), Pd(PPh₃)₄ (0.09 g, 0.075 mmol) was dissolved in 50 mL ACN/H₂O (v/v = 3: 2). Then the reaction mixture was degassed for 3 times, heated at 90 ºC in an oil bath and stirred under nitrogen for 24 h. The mixture was cooled to room temperature, filtered, and evaporated to remove ACN. The residue was diluted with 30 mL H₂O and then extracted with ethyl acetate (30 mL×3). The combined organic layer was washed with brine, dried over Na₂SO₄ for overnight, filtered, and concentrated *in vacuo* to give the crude product, which was isolated by flash chromatography on silica gel (EtOAc) to obtain the title compound (0.12 g, 19%). Mp 291□292ºC, EI-MS (m/z): 418.15 [M+H]⁺, 416.10 [M-H]⁻. ¹H NMR (400 MHz, DMSO-*d₆*) δ 11.83 (s, 1H), 7.99 (d, *J* = 8.2 Hz, 2H), 7.96 - 7.92 (m, 2H), 7.58 (d, *J* = 8.2 Hz, 2H), 7.35 - 7.28 (m, 4H), 6.85 (dd, *J* = 5.4, 2.4 Hz, 1H), 4.32 (s, 2H), 3.47 (s, 4H). ¹³C NMR (101 MHz, DMSO-*d₆*) δ 166.71, 165.92, 163.05, 148.44, 142.49, 142.39, 135.20, 133.97, 131.48, 130.36, 130.27, 129.25, 127.79, 126.70, 119.85, 115.76, 115.54, 110.69, 109.86.

The compounds **Y2**-**Y5** were prepared using the same procedure as described above, with 4-iodo-*1H*-indazol-3-amine (**1**) (1.5 mmol) and various boronic acid (**3b-3e**) (1.8 mmol) as starting materials.

5.1.9. 4-(3-amino-1H-indazol-4-yl)-N-(2-(4-bromobenz-amido) ethyl)benzamide (Y2)

Yield 0.20 g, 28%. Mp 300~302ºC; EI-MS (m/z) 476.05[M-H]⁻. ¹H NMR (400 MHz, DMSO-*d₆*) δ 11.83 (s, 1H), 7.98 (d, *J* = 8.2 Hz, 2H), 7.81 (d, *J* = 8.5 Hz, 2H), 7.70 (d, *J* = 8.5 Hz, 2H), 7.57 (d, *J* = 8.2 Hz, 2H), 7.35 - 7.27 (m, 2H), 6.85 (dd, *J* = 5.4, 2.4 Hz, 1H), 4.32 (s, 2H), 3.47 (s, 4H). ¹³C NMR (101 MHz, DMSO-*d₆*) δ 166.71, 166.05, 148.42, 142.50, 142.39, 135.21, 134.13, 133.97, 131.77, 129.84, 129.25, 127.80, 126.71, 125.34, 119.85, 110.69, 109.86.

5.1.10. 4-(3-amino-1H-indazol-4-yl)-N-(2-(4-methylbenzamido) ethyl)benzamide (Y3)

Yield 0.43 g, 69%. Mp 232□234ºC, EI-MS (m/z): 414.15 [M+H]⁺, 412.15 [M-H]⁻. ¹H NMR (400 MHz, DMSO-*d₆*) δ 11.83 (s, 1H), 7.99 (d, *J* = 8.1 Hz, 2H), 7.77 (d, *J* = 8.0 Hz, 2H), 7.57 (d, *J* = 8.0 Hz, 2H), 7.30 (dd, *J* = 17.4, 6.6 Hz, 4H), 6.85 (dd, *J* = 5.2, 2.1 Hz, 1H), 4.32 (s, 2H), 3.47 (s, 4H), 2.36 (s, 3H). ¹³C NMR (101 MHz, DMSO-*d₆*) δ 166.89, 166.70, 148.41, 142.50, 142.38, 141.44, 135.20, 133.96, 132.19, 129.25, 127.79, 127.70, 126.71, 119.86, 110.69, 109.86, 21.42.

5.1.11. N-(2-(4-(3-amino-1H-indazol-4-yl)benzamido) ethyl)-4-chloro-3(trifluoromethyl)benzamide (Y4)

Yield 0.61 g, 81%. Mp 284□286ºC, EI-MS (m/z): 502.10 [M+H]⁺, 500.10 [M-H]⁻. ¹H NMR (400 MHz, DMSO-*d₆*) δ 11.83 (s, 1H), 8.31 (s, 1H), 8.16 (d, *J* = 8.4 Hz, 1H), 7.98 (d, *J* = 8.3 Hz, 2H), 7.89 (d, *J* = 8.4 Hz, 1H), 7.57 (d, *J* = 8.3 Hz, 2H), 7.36 - 7.28 (m, 2H), 6.85 (dd, *J* = 5.4, 2.4 Hz, 1H), 4.32 (s, 2H), 3.49 (s, 4H). ¹³C NMR (101 MHz, DMSO-*d₆*) δ 166.73, 164.68, 148.43, 142.49, 142.42, 135.19, 134.32, 133.94, 133.40, 132.37, 129.24, 127.79, 126.88, 126.71, 124.51, 121.79, 119.85, 110.69, 109.87, 22.98.

5.1.12. 4-(3-amino-1H-indazol-4-yl)-N-(2-(4-(dimethylamino) benzamido)ethyl)benzamide (Y5)

Yield 0.18 g, 27%. Mp 279□281ºC, EI-MS (m/z): 443.15 [M+H]⁺, 441.10 [M-H]⁻. HRMS (ESI): calcd for [M+H]⁺ C₂₅H₂₇N₆O₂: 443.2195, found 443.0052. ¹H NMR (400 MHz, DMSO-*d6*) δ 11.84 (s, 1H), 7.99 (d, *J* = 8.0 Hz, 2H), 7.74 (d, *J* = 8.8 Hz, 3H), 7.57 (d, *J* = 8.1 Hz, 2H), 7.32 (d, *J* = 5.2 Hz, 2H), 6.88 - 6.83 (m, 1H), 6.71 (d, *J* = 8.8 Hz, 2H), 4.33 (s, 2H), 3.44 (s, 4H), 2.96 (s, 6H).

5.1.13. 6-bromo-1H-indazol-3-amine (4)

4-bromo-2-fluorobenzonitrile (5.0 g, 25.1 mmol) was dissolved in 1-butanol (20 mL), then followed by the addition of hydrazine monohydrate (1.0 mL, 50.3 mmol). The reaction mixture was heated to reflux for 4 h. Then cooled to room temperture, filtered, washed with n-hexane and dried to give **4** as white solid (4.77 g, 85%).

The compounds **Y6**-**Y10** were prepared using the same procedure as compound **Y1**, with 6-bromo-*1H*-indazol-3-amine (**4**) (1.5 mmol) and various boronic acids (**3a-3e**)

(1.8 mmol) as starting materials.

5.1.14. 4-(3-amino-1H-indazol-6-yl)-N-(2-(4-fluorobenzamido)ethyl)benzamide (Y6)

Yield 0.24 g, 38%. Mp 277□279ºC, HRMS (ESI): calcd for [M+H]⁺ $C_{23}H_{21}FN_5O_2$: 418.1679, found 418.1669. ^{1}H NMR (400 MHz, DMSO-d_6) δ 11.52 (s, 1H), 8.68 (d, J = 3.6 Hz, 2H), 7.93 - 7.97 (m, 4H), 7.83 - 7.75 (m, 2H), 7.50 (s, 1H), 7.38 - 7.20 (m, 3H), 5.43 (s, 2H), 3.47 (s, 4H).

5.1.15. 4-(3-amino-1H-indazol-6-yl)-N-(2-(4-bromobenzamido)ethyl)benzamide (Y7)

Yield 0.20 g, 29%. Mp 239□241ºC, HRMS (ESI): calcd for [M-H]⁻ $C_{23}H_{19}BrN_5O_2$: 476.0722, found 476.9787. ^{1}H NMR (400 MHz, DMSO-d_6) δ 9.96 (s, 1H), 8.69 (s, 1H), 8.36 (s, 1H), 7.81 (s, 1H), 7.78 (s, 1H), 7.73 (s, 1H), 7.70 (d, J = 2.8 Hz, 2H), 7.68 (s, 1H), 6.80 (s, 1H), 6.78 (s, 1H), 3.42 - 3.39 (m, 4H).

5.1.16. 4-(3-amino-1H-indazol-6-yl)-N-(2-(4-methylbenzamido)ethyl)benzamide (Y8)

Yield 0.14 g, 22%. Mp 172□174ºC, HRMS (ESI): calcd for [M+H]⁺ $C_{24}H_{24}N_5O_2$: 414.1930, found 414.1925. ^{1}H NMR (400 MHz, DMSO-d_6) δ 8.54 (d, J = 5.5 Hz, 1H), 8.22 (s, 1H), 7.83 (dd, J = 21.8, 8.1 Hz, 2H), 7.71 - 7.76 (m, 4H), 7.27 (d, J = 8.0 Hz, 2H), 6.79 (d, J = 8.7 Hz, 1H), 3.40 - 3.44 (m, 4H), 2.35 (s, 3H).

5.1.17. N-(2-(4-(3-amino-1H-indazol-6-yl)benzamido)ethyl)-4-chloro-3(trifluoromethyl)benzamide (Y9)

Yield 0.29 g, 38%. Mp 256□258ºC, HRMS (ESI): calcd for [M+H]⁺ $C_{24}H_{20}ClF_3N_5O_2$: 502.1258, found 502.1285. ^{1}H NMR (400 MHz, DMSO-d_6) δ 11.52 (s, 1H), 8.99 (s, 1H), 8.70 (s, 1H), 8.31 (s, 1H), 8.16 (d, J = 7.3 Hz, 1H), 7.95 (d, J = 7.0 Hz, 2H), 7.89 (d, J = 7.8 Hz, 1H), 7.80 (d, J = 6.2 Hz, 3H), 7.50 (s, 1H), 7.27 (d, J = 8.2 Hz, 1H), 5.43 (s, 2H), 3.49 (s, 4H).

5.1.18. 4-(3-amino-1H-indazol-6-yl)-N-(2-(4-(dimethylamino)benzamido)ethyl)benzamide (Y10)

Yield 0.26 g, 40%. Mp 271□273ºC, HRMS (ESI): calcd for [M+H]⁺ $C_{25}H_{27}N_6O_2$: 443.2195, found 443.2189. ^{1}H NMR (400 MHz, DMSO-d_6) δ 7.96 (d, J = 8.4 Hz, 2H), 7.78 - 7.81 (m, 3H), 7.74 (d, J = 9.0 Hz, 2H), 7.50 (s, 1H), 7.27 (dd, J = 8.4, 1.4 Hz, 1H), 6.71 (d, J = 9.0 Hz, 2H), 5.43 (s, 2H), 3.44 (s, 4H), 2.97 (s, 6H).

5.1.19. (4-fluorophenyl)(piperazin-1-yl)methanone (5a)

Trimethylacetyl chloride (2.42 mL, 20 mmol) and Et₃N (4.60 mL, 30 mmol) were added to a mixture of 4-fluorobenzoic acid (20 mmol) in dry CH_2Cl_2 (80 mL). The resulting mixture was stirred at room temperature for 0.5-1 h until a clear solution was observed. A solution of piperazine (3.44 g, 40 mmol) in EtOH (80 mL) was added, and the mixture was further stirred for 3 h. Then the reaction solution was evaporated to remove solvents. The residue was dissolved in 20 mL H_2O, and concd HCl (4 mL) was added. The resulting mixture was extracted with CH_2Cl_2 (5 mL) to remove bisadduct. NaOH (8 g) was added to the aqueous solution and then extracted with CH_2Cl_2 (30 mL × 3). The organic extract was further washed with H_2O (30 mL) and then dried over Na_2SO_4. Evaporation of the solvent at reduced pressure yielded the residue which was further used in next step. EI-MS (m/z) 208[M]⁺.

The intermediates **5b-5e** were prepared by commercially benzoic acids bearing different substituents and piperazine using the same method as described above.

The intermediates **6a-6e** was obtained using the same method as described for the preparation of compound **3a**, with 4-carboxyphenylboronic acid (6 mmol) and corresponding monoacylated piperazine **5a-5e** (7.2 mmol) as starting materials.

5.1.20. (4-(4-(4-fluorobenzoyl)piperazine-1-carbonyl)phenyl)boronic acid (6a)

(4-fluorophenyl)(piperazin-1-yl)methanone (**5a**) as starting materials. Yield 1.28 g, 60%. Mp 224□226ºC, EI-MS (m/z): 357.15 [M+H]⁺, 355.10 [M-H]⁻.

5.1.21. (4-(4-(4-bromobenzoyl)piperazine-1-carbonyl)phenyl)boronic acid (6b)

(4-bromophenyl)(piperazin-1-yl)methanone (**5b**) as starting materials. Yield 2.04 g, 82%. Mp 220□222ºC, EI-MS (m/z): 415.05 [M-H]⁻。

5.1.22. (4-(4-(4-methylbenzoyl)piperazine-1-carbonyl)phenyl)boronic acid (6c)

piperazin-1-yl(p-tolyl)methanone (**5c**) as starting materials.

13

Yield 2.0 g, 80%. Mp 209□211ºC, EI-MS (m/z): 351.15 [M-H]⁻.

5.1.23. (4-(4-(4-chloro-3-(trifluoromethyl)benzoyl) piperazine-1-carbonyl)phenyl)boronic acid (6d)

(4-chloro-3-(trifluoromethyl)phenyl)(piperazin-1-yl) meth-aneone (**5d**) as starting materials. Yield 2.19 g, 83%. Mp 156□158ºC, EI-MS (m/z): 441.10 [M+H]⁺.

5.1.24. (4-(4-(4-(dimethylamino)benzoyl)piperazine-1-carbonyl) phenyl)boronic acid (6e)

(4-(dimethylamino)phenyl)(piperazin-1-yl)methanone (**5e**) as starting materials. Yield 1.48 g, 65%. Mp 208□210ºC, EI-MS (m/z): 382.10 [M+H]⁺, 380.05 [M-H]⁻.

The compounds **Y11**-**Y15** were prepared using the same procedure as compound **Y1**, with 4-iodo-*1H*-indazol-3-amine (**1**) (1.5 mmol) and various boronic acid (**6a-6e**) (1.8 mmol) as starting materials.

5.1.25. (4-(4-(3-amino-1H-indazol-4-yl)benzoyl)piperazin-1-yl)(4-fluorophenyl)methanone (Y11)

Yield 0.31 g, 47%. Mp 283□285ºC, EI-MS (m/z): 444.02 [M+H]⁺, 442.15 [M-H]⁻. ¹H NMR (400 MHz, DMSO-d_6) δ 11.83 (s, 1H), 7.56 (s, 4H), 7.54 - 7.51 (m, 2H), 7.32 (s, 1H), 7.32 - 7.30 (m, 2H), 7.29 (d, J = 3.1 Hz, 1H), 6.88 - 6.82 (m, 1H), 4.36 (s, 2H), 3.68 - 3.49 (m, 8H). ¹³C NMR (101 MHz, DMSO-d_6) δ 169.55, 168.83, 164.32, 161.87, 148.45, 142.55, 140.95, 135.24, 135.04, 132.45, 130.21, 130.13, 129.41, 127.73, 126.72, 119.90, 116.03, 115.81, 110.65, 109.80, 60.37, 28.54, 21.53, 14.53.

5.1.26. (4-(4-(3-amino-1H-indazol-4-yl)benzoyl)piperazin-1-yl)(4-bromophenyl)methanone (Y12)

Yield 0.18 g, 24%. Mp 277□279ºC, EI-MS (m/z): 504.10 [M+H]⁺, 502.15 [M-H]⁻. ¹H NMR (400 MHz, DMSO-d_6) δ 11.83 (s, 1H), 7.72 - 7.63 (m, 2H), 7.56 (s, 4H), 7.41 (d, J = 7.7 Hz, 2H), 7.32 (d, J = 2.2 Hz, 2H), 6.87 - 6.83 (m, 1H), 4.36 (s, 2H), 3.65 - 3.49 (m, 8H).

5.1.27. (4-(4-(3-amino-1H-indazol-4-yl)benzoyl)piperazin-1-yl)(p-tolyl)methanone (Y13)

Yield 0.57 g, 86%. Mp 259□261ºC, EI-MS (m/z): 440.20 [M+H]⁺, 438.20 [M-H]⁻. ¹H NMR (400 MHz, DMSO-d_6) δ 11.82 (s, 1H), 7.56 (s, 4H), 7.38 - 7.30 (m, 4H), 7.27 (d, J = 7.7 Hz, 2H), 6.87 - 6.82 (m, 1H), 4.35 (s, 2H), 3.65 -

3.51 (m, 8H), 2.35 (s, 3H). ¹³C NMR (101 MHz, DMSO-d_6) δ 171.94, 169.84, 169.53, 148.38, 142.54, 140.86, 139.88, 135.24, 135.06, 133.13, 129.40, 127.66, 126.72, 119.89, 110.65, 109.79, 28.47, 22.98, 21.38.

5.1.28. (4-(4-(3-amino-1H-indazol-4-yl)benzoyl)piperazin-1-yl)(4-chloro-3-(trifluoromethyl)phenyl)Methanone (Y14)

Yield 0.30 g, 38%. Mp 253□255ºC, EI-MS (m/z): 528.10 [M+H]⁺, 526.15 [M-H]⁻. ¹H NMR (400 MHz, DMSO-d_6) δ 11.83 (s, 1H), 7.92 (s, 1H), 7.85 - 7.77 (m, 2H), 7.56 (s, 4H), 7.32 (s, 1H), 7.31 (d, J = 2.2 Hz, 1H), 6.85 (s, 1H), 4.35 (s, 2H), 3.90 - 3.39 (m, 8H). ¹³C NMR (101 MHz, DMSO-d_6) δ 169.57, 167.28, 148.45, 142.54, 140.97, 135.71, 135.19, 135.01, 133.17, 132.38, 129.41, 127.67, 127.17, 126.72, 124.38, 121.67, 119.89, 110.65, 109.80, 60.30, 28.47, 21.24, 14.55, 12.93.

5.1.29. (4-(4-(3-amino-1H-indazol-4-yl)benzoyl)piperazin-1-yl)(4-(dimethylamino)phenyl)methanone (Y15)

Yield 0.20 g, 28%. Mp 282□284ºC, EI-MS (m/z): 469.29 [M+H]⁺, 467.15 [M-H]⁻. HRMS (ESI): calcd for [M+H]⁺ $C_{27}H_{29}N_6O_2$: 469.2352, found 469.0079. ¹H NMR (400 MHz, DMSO-d_6) δ 11.83 (s, 1H), 7.56 (s, 4H), 7.33 (d, J = 7.4 Hz, 4H), 6.85 (s, 1H), 6.72 (d, J = 8.2 Hz, 2H), 4.36 (s, 2H), 3.59 (s, 8H), 2.96 (s, 6H).

The compounds **Y16**-**Y20** were prepared using the same procedure as compound **Y1**, with 6-bromo-*1H*-indazol-3-amine (**4**) (1.5 mmol) and various boronic acid (**6a-6e**) (1.8 mmol) as starting materials.

5.1.30. (4-(4-(3-amino-1H-indazol-6-yl)benzoyl)piperazin-1-yl)(4-fluorophenyl)methanone (Y16)

Yield 0.24 g, 36%. Mp 257□259ºC, HRMS (ESI): calcd for [M+H]⁺ $C_{25}H_{23}FN_5O_2$: 444.1836, found 444.1831. ¹H NMR (400 MHz, DMSO-d_6) δ 11.52 (s, 1H), 7.78 (d, J = 8.2 Hz, 3H), 7.63 - 7.42 (m, 5H), 7.36 - 7.16 (m, 3H), 5.42 (s, 2H), 3.49 - 3.67 (m, 8H).

5.1.31. (4-(4-(3-amino-1H-indazol-6-yl)benzoyl)piperazin-1-yl)(4-bromophenyl)methanone (Y17)

Yield 0.30 g, 40%. Mp 134□136ºC, HRMS (ESI): calcd for [M+H]⁺ $C_{25}H_{23}BrN_5O_2$: 504.1035, found 504.1029. ¹H NMR (400 MHz, DMSO-d_6) δ 7.78 (d, J = 7.1 Hz, 3H), 7.68 (d, J = 5.9 Hz, 3H), 7.53 (d, J = 8.5 Hz, 2H), 7.47 (s,

1H), 7.41 (d, *J* = 6.4 Hz, 2H), 5.41 (s, 2H), 3.68 - 3.44 (m, 8H).

*5.1.32. (4-(4-(3-amino-1H-indazol-6-yl)benzoyl)piperazin-1-yl)(p-tolyl)methanone (**Y18**)*

Yield 0.21 g, 32%. Mp 244□246ºC, HRMS (ESI): calcd for [M+H]$^+$ C$_{26}$H$_{26}$N$_5$O$_2$: 440.2087, found 440.2085. ^{1}H NMR (400 MHz, DMSO-*d$_6$*) δ 11.52 (s, 1H), 7.78 (d, *J* = 8.2 Hz, 3H), 7.53 (d, *J* = 8.0 Hz, 2H), 7.47 (s, 1H), 7.34 (d, *J* = 7.8 Hz, 2H), 7.30 - 7.22 (m, 3H), 5.42 (s, 2H), 3.50 - 3.65 (m, 8H), 2.35 (s, 3H).

*5.1.33. (4-(4-(3-amino-1H-indazol-6-yl)benzoyl)piperazin-1-yl)(4-chloro-3-(trifluoromethyl)phenyl)methanone (**Y19**)*

Yield 0.16 g, 20%. Mp 224□226ºC, HRMS (ESI): calcd for [M]$^+$ C$_{26}$H$_{21}$ClF$_3$N$_5$O$_2$: 527.1336, found 527.0687. ^{1}H NMR (400 MHz, DMSO-*d$_6$*) δ 8.45 (s, 1H), 8.30 (s, 1H), 8.18 (d, *J* = 8.2 Hz, 1H), 7.90 - 7.75 (m, 5H), 7.37 (d, *J* = 8.0 Hz, 2H), 3.61 - 3.37 (m, 8H).

*5.1.34. (4-(4-(3-amino-1H-indazol-6-yl)benzoyl)piperazin-1-yl)(4-(dimethylamino)phenyl)methanone (**Y20**)*

Yield 0.29 g, 41%. Mp 200□203ºC, HRMS (ESI): calcd for [M+H]$^+$ C$_{27}$H$_{29}$N$_6$O$_2$: 469.2352, found 469.2342. ^{1}H NMR (400 MHz, DMSO-*d$_6$*) δ 7.78 (d, *J* = 8.2 Hz, 3H), 7.53 (d, *J* = 8.3 Hz, 2H), 7.47 (s, 1H), 7.32 (d, *J* = 8.8 Hz, 2H), 7.24 (dd, *J* = 8.4, 1.3 Hz, 1H), 6.72 (d, *J* = 8.9 Hz, 2H), 5.42 (s, 2H), 3.575 - 3.59 (m, 8H), 2.96 (s, 6H).

5.2. In vitro kinase assays

Kinase inhibition assays were performed using ADP-Glo^{TM} kinase assay kit from Promega (Madison, WI) according to the manufacturer's instructions, with Imatinib as the positive control. General procedures were as following: Kinase was incubated with the corresponding substrate /ATP mixture and inhibitors in a final buffer of Tris 40 mM (pH 7.4), MgCl$_2$ 10 mM, BSA 0.1mg/mL, DTT 1mM with a total volume of 5 μL in a 384-well plate, and the kinase reaction proceeded at 30□ for 60 min. Then 5 μL ADP-Glo^{TM} reagent was added and incubated at room temperature for 40 min, in order to terminate the kinase reaction and consume the remaining ATP. Next, 10 μL kinase detection reagent was added to convert ADP to ATP, and introduced luciferase/luciferin to detect ATP. At

this step, the plate was incubated at room temperature for 30 min, and the luminescence was measured by VICTOX X multiple plate reader. The luminescence signal is proportional to the amount of ATP present and inversely correlated to kinase activity.

5.3 Cell growth inhibition assays

The MTT assays were performed to evaluate the antiproliferative activity and identify the cytotoxicity of the title compounds *in vitro*. Imatinib was used as the positive control. The K562R cells expressing T315I mutation was kindly provided by Professor Libo Yao (Fourth Military Medical University, Xi'an, China). The Hek293 cells was provided by Dr. Tao Zhang (Xi'an Jiaotong University, Xi'an, China). The EA.hy926 cells was provided by Dr. Wen Lu (Xi'an Jiaotong University, Xi'an, China). The cancer cell lines (K562 and K562R cells) were cultured in RPMI 1640 medium with 10% fetal bovine serum (FBS). The two normal human cells (Hek293 and EA.hy926 cells) were cultured in DMEM medium with 10% FBS.

The cells were seeded into 96-well microtiter plates (2500 cells in 180 μl of nutrient medium per well), and incubated in 5% CO$_2$ at 37 °C for 12 h. The tested compounds (20 μl) at the indicated final concentrations were added to the culture medium and incubated for 48 h. Fresh MTT was added to each well at the final concentration of 0.5 mg/mL, and incubated with cells at 37°C for 4 h. Then aspirate the supernatant, and add 150 μL DMSO to each well. The absorbance values were determined by a microplate reader (Bio-Rad, Hercules, CA, USA) at 490 nm. The IC$_{50}$ values were calculated according to inhibition ratios.

5.4 Western blot assay

K562 cells were treated with vehicle (DMSO) or drug at desired concentration for 4 h. The cells were lysed in SDS sample buffer, collected, and normalized using BCA protein assay kit before being diluted in SDS loading buffer. Then the samples containing equal amounts of protein were separated by SDS-PAGE. After electrophoresis, proteins were transferred to PVDF membranes and blocked with 5% nonfat milk in Tris-buffered saline with 0.1% Tween-20. Membranes were

incubated with antibodies Bcr-Abl, p-Bcr-Abl, and actin at 4□ overnight. The membranes were washed with PBS three times, and incubated with the appropriate anti-HRP secondary antibodies for 2 h at room temperature. Finally, immunoreactive proteins were visualized using the enhanced chemiluminescence system from Pierce Chemical.

5.5 Molecular docking study

In order to investigate the binding mode of the title compounds with both Bcr-Abl^{WT} and Bcr-Abl^{T315I}, molecule docking was performed using Surflex-Dock Module of Sybyl-X 2.0. The molecules were drawn with Sketch and minimized by Powell's method for 1000 iterations under Tripos Force field with Gasteiger-Huckel charge. Crystal structures of Bcr-Abl^{WT} (PDB ID: 1IEP) and Bcr-Abl^{T315I} (PDB ID: 3QRJ) were imported, and corresponding ligand was used to define the binding cavity and generate the promotal. The ligands and water molecules were removed and hydrogen was added and minimized using Tripos force field and Pullman charges. The residues in a radius 5.0Å around ligands were selected as active site. The other docking parameters were kept at default. The inhibitors were docked into the active site using ligand-based mode.

Acknowledgment

References

1. C.L. Sawyers, A. Houchhaus, E. Feldman, J.M. Goldman, C.B. Miller, O.G. Ottmann, C.A. Schiffer, M. Taipaz, F. Guilhot, M.W. Deininger, T. Fischer, S.G. O'Brien, R.M. Stone, C.B. Gambacorti- Passerini, N.H. Russell, J.J. Reiffers, T.C. Shea, B. Chapuis, S. Cout, S. Tura, E. Morra, R.A. Larson, A. Saven, C. Peschel, A. Gratwohl, F. Mandelli, M. Ben-Am, I. Gathmann, R. Capdeville, R.L. Paquette, B.J. Druker, Imatinib induces hematologic and cytogenetic responses in patients with chronic myelogenous leukemia in myeloid blast crisis: results of a phase II study, Blood 99(2002) 3530-3539.

2. E.K. Greuber, P. Smith-Pearson, J. Wang, A.M. Pendergast, Role of ABL family kinases in cancer: from leukaemia to solid tumors, Nat. Rev. Cancer 13(2013) 559-571.

3. A. Quintas-Cardama, J. Cortes, Molecular biology of bcr-abl1-positive chronic myeloid leukemia, Blood 113(2009) 1619-1630.

4. R. Capdeville, E. Buchdunger, J. Zimmermann, A. Matter, Glivec (STI571, Imatinib), a rationally developed, targeted anticancer drug, Nat. Rev. Drug Discov. 1(2002) 493-502.

5. P. Gupta, R.J. Kathawata, L. Wei, F. Wang, X. Wang, B.J. Druker, L.W. Fu, Z.S. Chen, PBA2, a novel inhibitor of imatinib-resistant BCR-ABL T315I mutation in chronic myeloid leukemia, Cancer Lett. 383(2016), 220-229.

6. J.Y. Blay, M. von Mehren, Nilotinib: a novel, selective tyrosine kinase inhibitor, Semin. Oncol. 38(2011) S3-S9.

7. N.P. Shah, C. Tran, F.Y. Lee, P. Chen, D. Norris, C.L. Sawyers, Overriding imatinib resistance with a novel ABL kinase inhibitor, Science 305(2004) 399-401.

8. L. Stansfield, T.E. Hughes, T.L. Walsh-Chocolaad, Bosutinib: a second-generation tyrosine kinase inhibitor for chronic myelogenous leukemia, Ann. Pharmacother 47(2013) 1703-1711.

9. H.N. Banayath, O.P. Sharma, M.S. Kumar, R. Baskaran, identification of novel tyrosine kinase inhibitors for drug resistant T315I mutant BCR-ABL: a virtual screening and molecular dynamics simulations study, Sci. Rep. 4(2014) 6948.

10. T. O'Hare, W.C. Shakespeare, X. Zhu, C.A. Eide,

V.M. Rivera, F. Wang, L.T. Adrian, T. Zhou, W.S. Huang, Q. Xu, C.A. 3rd Metcalf, J.W. Tyner, M.M. Loriaux, A.S. Corbin, S. Wardwell, Y. Ning, J.A. Keats, Y. Wang, R. Sundaramoorthi, M. Thomas, D. Zhou, J. Snodgrass, L. Commodore, T.K. Sawyer, D.C. Dalgarno, M.W. Deininger, B.J. Druker, T. Clackson, AP24534, a pan-BCR-ABL inhibitor for chronic myeloid leukemia, potently inhibits the T315I mutant and overcomes mutation-based resistance, Cancer Cell 16(2009) 401-412.

11. U.S. Food and Drug Administration. FDA Drug Safety Communication: FDA asks manufacturer of the leukemia drug Iclusig (ponatinib) to suspend marketing and sales. http://www.fda.gov/Drugs/DrugSafety/ucm 373040.htm (accessed May 26, 2015).

12. B. Okram, A. Nagle, F.J. Adrian, C. Lee, P. Ren, X. Wang, T. Sim, Y. Xie, X. Wang, G. Xia, G. Spraggon, M. Warmuth, Y. Liu, N.S. Gray, A general strategy for creating "inactive-confirmation" abl inhibitors, Chem. Biol. 13(2006) 779-786.

13. X. Pan, J. Dong, Y. Shi, R. Shao, F. Wei, J. Wang, J. Zhang, Discovery of novel Bcr-abl inhibitors with diacylated piperazine as the flexible linker, Org. Biomol. Chem, 13(2015) 7050-7066.

14. Y. Luo, F. Jiang, T.B. Cole, V.P. Hradil, D. Reuter, A. Chakravartty, D.H. Albert, S.K. Davidsen, B.F. Cox, E.M. McKeegan, G.B. Fox, A novel multi-targeted tyrosine kinase inhibitor, linifanib (ABT-869), produces functional and structural changes in tumor vasculature in an orthotopic rat glioma model, Cancer Chemother. Pharmacol. 69(2012) 911-921.

15. Y. Shan, J. Dong, X. Pan, L. Zhang, J. Zhang, Y. Dong, M. Wang, Expanding the structural diversity of Bcr-Abl inhibitors: Dibenzoylpiperazin incorporated with 1H-indazol-3-amine, Eur. J. Med. Chem. 104(2015) 139-147.

16. A.W. Kruger, M.J. Rozema, A. Chu-kung, J. Gandarilla, A.R. Haight, B.J. Kotecki, S.M. Richter, A.M. Schwartz, Z. Wang, The discovery and development of a safe, practical synthesis of ABT-869, Org. Process Res. Dev. 13(2009) 1419-1425.

17. W.G. Kong, Y. Zhou, Q.L. Song, Lewis-acid promoted chemoselective condensation of 2-aminobenzimi-dazoles or 3-aminoindazoles with 3-ethoxycyclo-butanones to construct fused nitrogen heterocycles, Adv. Synth. Catal. 360(2018) 1943-1948.

18. S.K. Verma, R. Ghorpade, A. Pratap, M.P. Kaushik, CDI-mediated monoacylation of symmetrical diamines and selective acylation of primary amines of unsymmetrical diamines, Green Chem. 14(2012) 326-329.

19. D.W. 2nd Zehnder, D.B. Smithrud, Facile synthesis of rotaxanes through condensation reactions of DCC-[2]rotaxanes, Org. Lett. 3(2001) 2485-2487.

20. L. Lai, E. Wang, B.J. Luh, Reaction of piperazine with trimethylacetic arylcarboxylic anhydride; A convenient method for preparing monoacylated piperazine derivatives, Synthesis 3(2001) 361-363.

21. X. Pan, F. Wang, Y. Zhang, H. Gao, Z. Hu, S. Wang, J. Zhang, Design, synthesis and biological activities of Nilotinib derivates as antitumor agents, Bioorg. Med. Chem. 21(2013) 2527-2534.

22. H. Zegzouti, M. Zdanovskaia, K. Hsiao, S.A. Goueli, ADP-Glo: a Bioluminescent and homogeneous ADP monitoring assay for kinases, Assay Drug Dev. Technol. 7(2009) 560-572.

23. J. Dong, X. Pan, J. Wang, P. Su, L. Zhang, F. Wei, J. Zhang, Synthesis and biological evaluation of novel aromatic-heterocyclic biphenyls as potent anti-leukemia agents, Eur. J. Med. Chem. 101(2015) 780-789.

24. Y. Ru, Q. Wang, X. Liu, M. Zhang, D. Zhong, M. Ye, Y. Li, H. Han, L. Yao, X. Li, The chimeric ubiquitin ligase SH2-U-box inhibits the growth of imatinib-sensitive and resistant CML by targeting the native and T315I-mutant BCR-ABL, Sci. Rep. 6 (2016): 28352.

25. H.M. Revankar, M.V. Kulkarni, S.D. Joshi, U.A.

More, Synthesis, biological evaluation and docking studies of 4-aryloxymethyl coumarins derived from substructures and degradation products of vancomycin, Eur. J. Med. Chem. 70(2013) 750-757.

26. B. Nagar, W.G. Bornman, P. Oellicena, T. Schindler, D.R. Veach, W.T. Miller, B. Clarkson, J. Kuriyan, Crystal structures of the kinase domain of c-Abl in complex with the small molecule inhibitors PD173955 and imatinib (STI-571), Cancer Res. 62(2002) 4236-4243.

27. W.W. Chan, S.C. Wise, M.D. Kaufman, Y.M. Ahn, C.L. Ensinger, T. Haack, M.M. Hood, J. Jones, J.W. Lord, W.P. Lu, D. Miller, W.C. Patt, B.D. Smith, P.A. Petillo, T.J. Rutkoski, H. Telikepalli, L. Vogeti, T. Yao, L. Chun, R. Clark, P. Evangelista, L.C. Gavrilescu, K. Lazarides, V.M. Zaleskas, L.J. Stewart, R.A. Van Etten, D.L. Flynn, Conformational control inhibition of the BCR-ABL 1 tyrosine kinase, including the gatekeeper T315I mutant, by the switch-control inhibitor DCC-2036, Cancer Cell 19(2011) 556-568.

28. C.A. Rhodes, P.G. Dougherty, J.K. Cooper, Z. Qian, S. Lindert, Q.E. Wang, D. Pei, Cell-permeable bicyclic peptidyl inhibitors against NEMO-IκB kinase interaction directly from a combinatorial library, J. Am. Chem. Soc. 140(2018) 12102-12110.

Highlights

- ➢ Novel Bcr-Abl inhibitors with flexible linker to reduce steric clash with Ile315 in Bcr-Abl^{T315I} kinase.

- ➢ 6-phenyl-1H-indazol-3-amine is a promising hinge binding moiety.

- ➢ Compound **Y9** exhibited potent activity comparable to that of imatinib.